

Supplementary Information

Novel p-type and metallic dual-functional Cu-Al₂O₃ ultra-thin layers for the back electrode enabling high performance of thin film solar cells

Qinxian Lin[†], Yantao Su[†], Ming-Jian Zhang[†], Xiaoyang Yang, Sheng Yuan, Jiangtao Hu, Yuan Lin, Jun Liang and Feng Pan**

[†]These authors contributed equally to this work

1. Experimental Section

2. Performance characterization of CdTe cells with Cu/different thicknesses Al₂O₃ back contact;

3. (1) Capacitance-Voltage(CV) measurement for the p-type semiconductor;

(2) Voltage-Current characteristic of Cu-Al₂O₃ thin film;

4. The reaction of Cu/Al₂O₃ and the formation of interface;

5. The analysis of XPS for Cu-Al₂O₃ interface and Cu content in the CdTe devices;

6. The TEM image of Cu-Al₂O₃ thin film;

7. The analysis of EQE;

8. The solar cell performance with different Cu annealing treatment;

9. The FTO glass also impacts on the power conversion efficiency of CdTe solar cell.

1. Experimental Section

Methods: The CdTe cells were fabricated as follows. About 200-nm-thick CdS window layers were grown by radio frequency magnetron sputtering on the tFTO-coated soda-lime glass substrates, then CdTe absorber layer with the thickness of about 4-5 μm was deposited by close space sublimation (CSS). CdCl_2 thermal treatment was performed at 420 $^\circ\text{C}$ for 30 minutes following the CdTe deposition. The cells were etched in a phosphoric acid: nitric-acid: DI-water (NP) mixed solution to provide a clean Te-rich surface. Then the samples were transferred into the ALD system for ultrathin Al_2O_3 deposition. After that, Cu films with the thickness of 3-15 nm were evaporated. Different annealing temperature have been used for 30 minutes under N_2 atmosphere to make Cu diffusion through the ALD- Al_2O_3 layer, and the optimal one is 250 $^\circ\text{C}$ (seen in the SI). Finally 40-nm-thick Au layer was evaporated as back electrode. The cell was scribed to $0.5 \times 0.5 \text{ cm}^2$ area.

Characterization and measurements: PCE values were determined by J-V curve measurements (using a Keithley 2602A source meter) under a 1 sun illumination with AM 1.5 G spectrums from a solar simulator. The theoretical J_{sc} obtained by integrating the external quantum efficiency EQE under the AM 1.5G solar spectrum. In order to study the Cu diffusion mechanism, the electrical properties of Cu/ Al_2O_3 films were investigated by capacitance-voltage (CV), voltage-current (IV) characterization, the optical transmission spectra (UV-vis), and scanning electron microscope (SEM). X-ray photoelectron spectroscopy (XPS) measurements were carried out on a Thermo Fisher Scientific ESCALAB 250Xi system with a monochromated Al $K\alpha$ radiation. During the XPS data acquisition, the constant analyzer energy (CAE) mode was used at a step size of 0.1 eV. The carbon C-1s peak (284.8 eV) from the adventitious carbon was employed as the reference for binding

energy (BE) calibration. BE values of valence band spectrum for samples were corrected by Au foil mounted along with the samples. The peak contributions were extracted by combining a Lorentzian and a Gaussian function. The background was subtracted using Shirley function.

2. Performance characterization of CdTe cells with Cu/different thicknesses Al₂O₃ back contact.

Table S1. The photovoltaic parameters of CdTe solar cell with 2 nm-thickness of ALD-Al₂O₃.

CdTe cell with Cu	J _{sc} (mA/cm ²)	V _{oc} (mV)	FF	PCE (%)
STD	24.2	752	62	11.2
3nm	22.7	755	57	9.8
6nm	23.4	765	67	12.1
9nm	24.2	782	68	13.0
12nm	24.3	767	62	11.6
15nm	24.3	772	60	11.3

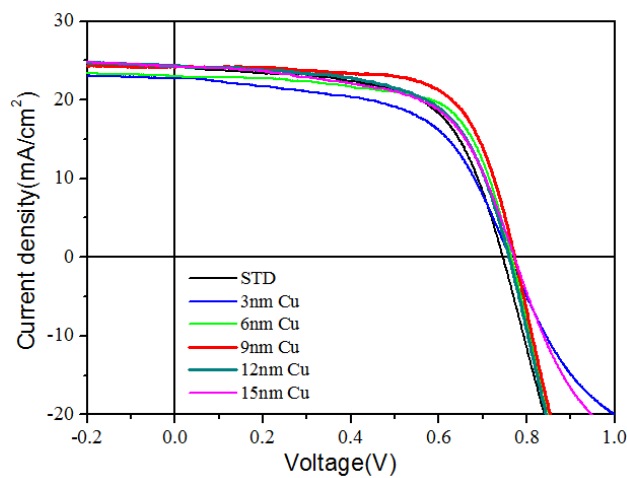


Figure S1. *J*–*V* characteristics of CdTe solar cells with different Cu thicknesses on 2 nm ALD-Al₂O₃.

Table S2. The photovoltaic parameters of CdTe solar cell with 1 nm-thickness of ALD-Al₂O₃.

CdTe cell				
with Cu	J_{sc}(mA/cm²)	V_{oc} (mV)	FF	PCE (%)
3 nm	23.9	750	0.63	11.2
6 nm	24.2	750	0.62	11.3
9 nm	24.8	735	0.53	9.7
15 nm	26.7	678	0.46	8.3

Table S3. The photovoltaic parameters of CdTe solar cell with 3 nm-thickness of ALD-Al₂O₃.

CdTe cell				
with Cu	J_{sc}(mA/cm²)	V_{oc} (mV)	FF	PCE (%)
9 nm	23.0	700	0.51	8.2
15 nm	23.2	710	0.57	9.2
25 nm	24.7	755	0.53	9.9

Table S4. The results of CdTe solar cell with different thickness of Al₂O₃ and Cu.

Cu	3 nm	6 nm	9 nm	15 nm	25 nm
Al₂O₃					
1 nm	11.2	11.3	9.7	8.3	
2 nm	9.9	12.1	13.0	11.3	
3 nm			8.2	9.2	9.9

From the J-V characteristics parameter list above, we can see when the thickness of Al_2O_3 is 1 nm, the performance of CdTe solar cells have not been greatly improved, which might account for inoperative ALD- Al_2O_3 layer. Because the Al_2O_3 layer is not thick enough to catch the excessive Cu; on the other hand, when the thickness of Al_2O_3 is more than 3 nm, the efficiency is degradation obviously. This can be explained by the photo current transport behavior, which can maintain a relative low resistance contact to the back of CdTe with the ultra-thin (≤ 2 nm) dielectrics of Al_2O_3 , but a thick (≥ 3 nm) would block the Cu diffusion so that build up high barrier and block the hole transportation.

3 . (1) Capacitance-Voltage(CV) measurement for the p-type semiconductor.

We use the structure of metal-insulation-semiconductor (MIS) to detect the CV characteristic.¹ First, the 10 nm Cu evaporate on the FTO glass, and then 5 nm Al_2O_3 is coated on Cu surface by atomic layer deposition and the 40 nm insulation layer is following. Finally, the Au electrode is evaporated on the device surface.

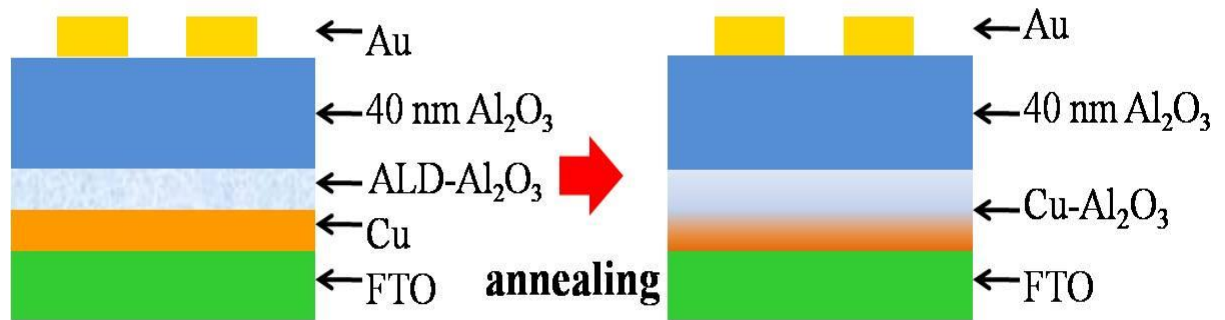


Figure S2. The diagram of our MIS device and the equivalent electronic circuits.

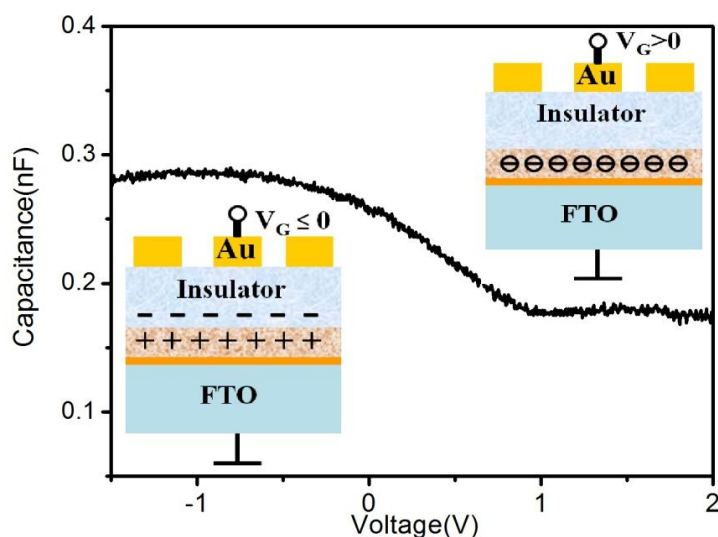


Figure S3. CV characterization and the device simulation of carriers transport.

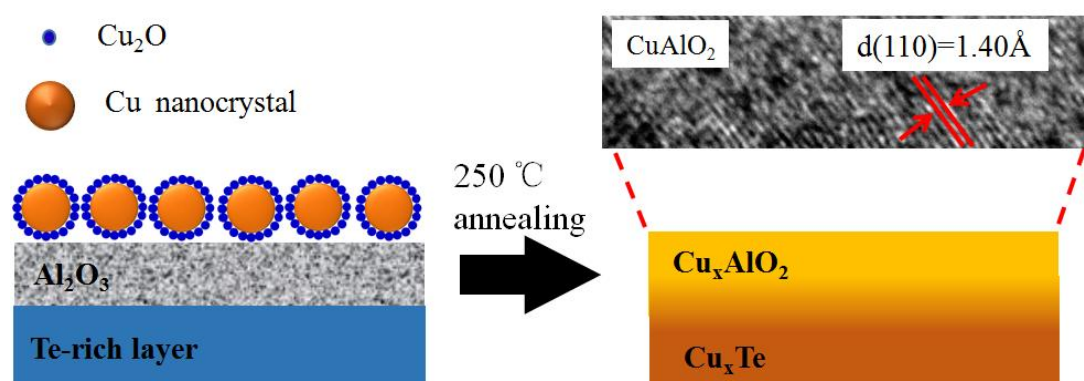


Figure S4. The schematic diagram of the reaction between Cu and Al_2O_3 on the surface of CdTe;

In our experiments, the thicknesses of ALD- Al_2O_3 film and Cu film are 2 nm and 9 nm, respectively. So it is easy to understand why Cu and Al_2O_3 would interdiffuse in a relatively low annealing temperature (250°C) and form a Cu- Al_2O_3 film. We have found the relevant reference to prove this formation mechanism. When depositing the Cu film in an atmosphere with little O_2 , Cu_2O would be formed on the surface of Cu nanocrystals into $\text{Cu}_2\text{O}@\text{Cu}$ core-shell nanoparticles. These nanoparticles would react with ALD- Al_2O_3 under 450°C , the reaction can be described as: $\text{Al}_2\text{O}_3 + \text{Cu}_2\text{O} \rightarrow 2 \text{CuAlO}_2$. So the whole reaction procedure could be illuminated in **Figure S4** above.

(2) Voltage-Current characteristic of Cu-Al₂O₃ thin film.

In order to evaluate the back contact conduction mechanism, we use the FTO/Al₂O₃/9 nm Cu structure to analyze by the IV curves, which can simulate the carriers transport at the back contact of our solar cell. After annealing in 250 °C, the resistance of 3 nm Al₂O₃ devices is obviously higher than the 2 nm ones (**Figure S5**), and the 2 nm devices show metal characteristic and 3 nm is more like semiconductor material at high temperature. From the CV and IV result, we can suppose the Cu diffusion is like **Figure S6**.

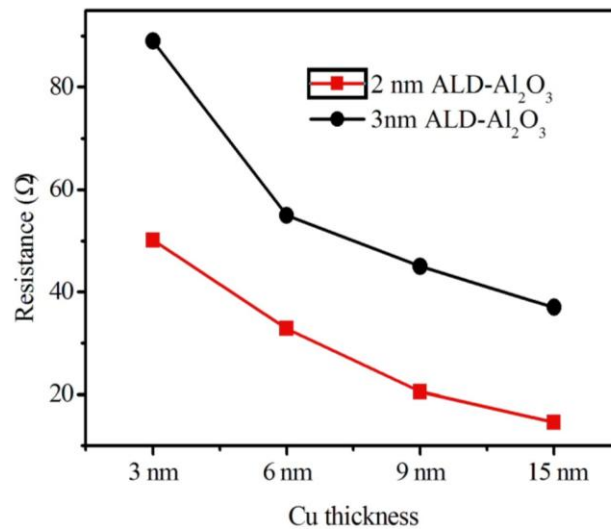


Figure S5. The resistance of 2 nm and 3 nm ALD-Al₂O₃ with different Cu thickness devices.

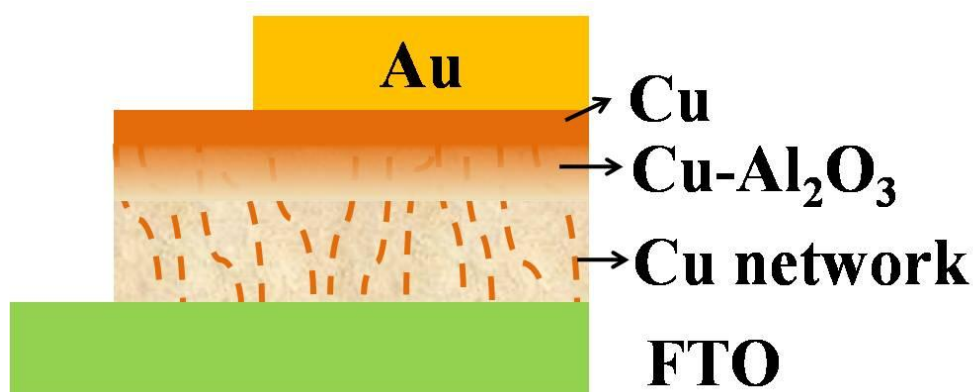


Figure S6. The diagram of Cu diffusion in the ALD-Al₂O₃ layer.

4. The reaction of Cu/Al₂O₃ and the formation of interface.

The optical transmission spectra can detect the transmittance of different growth temperature device. **Figure S7** presents the transmission spectra for the Cu-Al₂O₃ films grown at various growth temperatures from room temperature to 300 °C. The transmittance are over 75% in the visible region for the film grown Al₂O₃ at 300 °C, and show up an absorption edge at about 400nm, which is obviously different from the film grown at lower temperatures. This also shows the relationship between absorption coefficient as a function of photon energy.² A plot of $(\alpha h\nu)^2$ as a function of $h\nu$, where α is the absorption coefficient and $h\nu$ is the photon energy in eV, allows the optical band-edge absorption to be determined to be 2.7 eV.

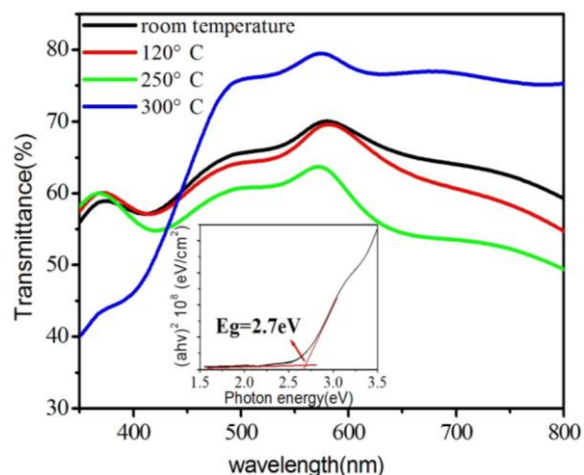


Figure S7. The transmission spectra of Cu/ Al₂O₃ films at various growth temperatures and the plot of $(\alpha h\nu)^2$ vs photon energy for Cu/ Al₂O₃ film grown at 300 °C

5. The analysis of XPS for Cu-Al₂O₃ interface and Cu content in the CdTe devices.

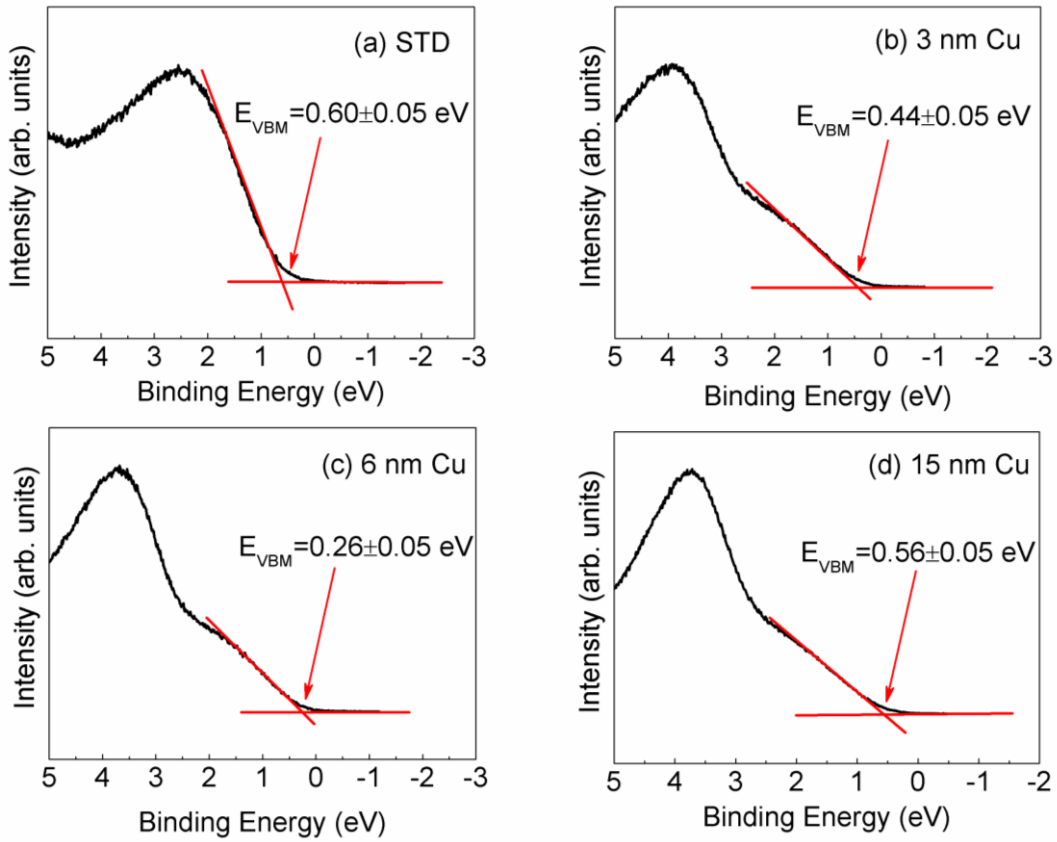


Figure S8. Valence band spectra for the STD and different thicknesses Cu cells (exclude the 9 nm Cu cell).

Cu thickness (nm)	STD	3	6	9	15
VBM (eV)	0.60	0.44	0.26	0.15	0.56
EV (eV)	...	0.16	0.34	0.45	0.04
EC (eV)	...	1.82	2.00	2.11	1.70

Table S5. The valence band maxima (VBM), valence band offset (E_V), and conduction band offset (E_C) were recorded for the STD and different thicknesses Cu cells. The energy origin is taken at the Fermi level position.

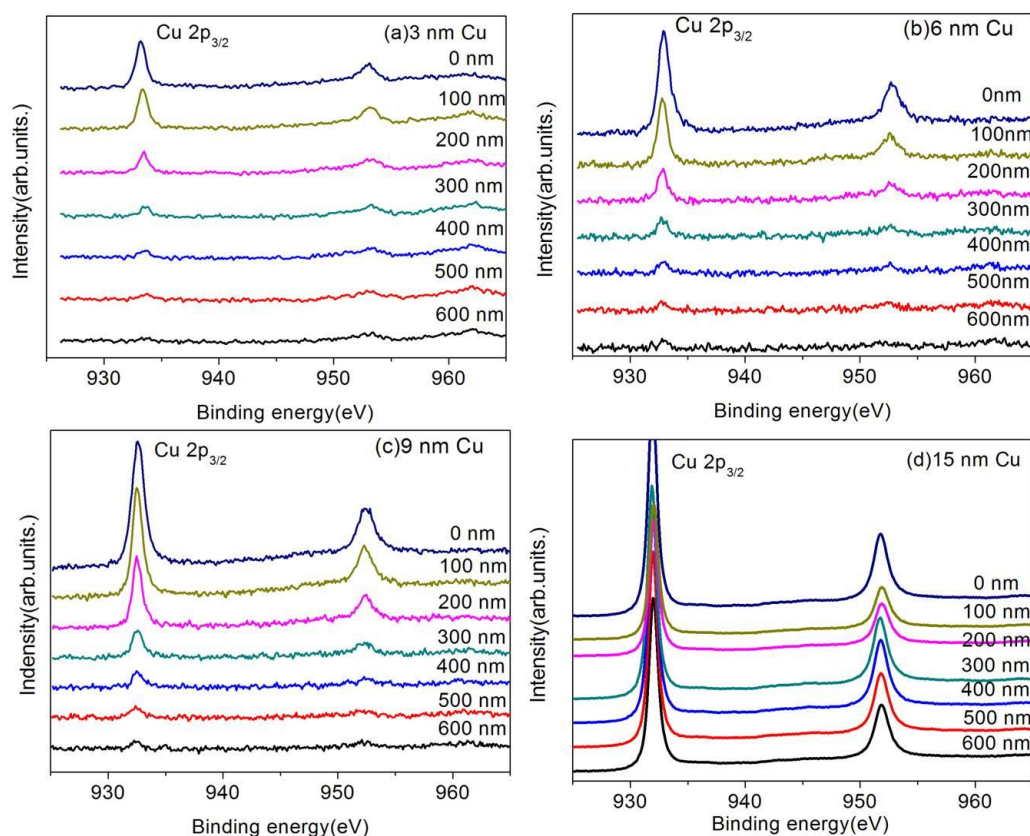


Figure S9. The depth profile of Cu $2p_{3/2}$ XPS spectra with Ar^+ etching for all cell with 2 nm ALD- Al_2O_3 .

In order to confirm our speculate above, the XPS depth profile was further performed to analyze the relative content of Cu in all the devices (shown in Figure 4c). When the thickness of Cu film is 3–9 nm, the Cu content significantly decreases in the first 50 nm, and then tends to be constant in the Cu_xTe layer. When the thickness of Cu film increases to 15 nm, its diffusion can not be efficiently controlled by the $\text{Cu-Al}_2\text{O}_3$ layer due to the large amount of excessive Cu, and the content of Cu maintains at a high level around the surface of the first 200 nm depth. So these excessive Cu could diffuse into the p-n junction (Figure S8), which greatly damaged the performance of CdTe cells. From Figure S8, we can see if the amount of Cu is not large (like 3, 6 and 9 nm), most of the Cu would be controlled by the ALD- Al_2O_3 and stayed at the top 200 nm of CdTe surface, little Cu could be detect after 300 nm. When the Cu thickness is larger than 15 nm (like the S8d), the Al_2O_3 layer could

not control Cu diffusion, so that there is still a high content of Cu at the 600 nm depth, which would diffuse into the CdTe/CdS pn junction and deteriorated the cells.

6. The TEM image of Cu- Al_2O_3 thin film.

Sample preparation: In order to observe the high-resolution TEM (HRTEM) of Cu- Al_2O_3 thin film, we use SiO_2 as a substrate for the sample. First, Cu was evaporated on the SiO_2 substrate, and then Al_2O_3 atomic layer was deposition and annealing at 250 °C for 30 mins.

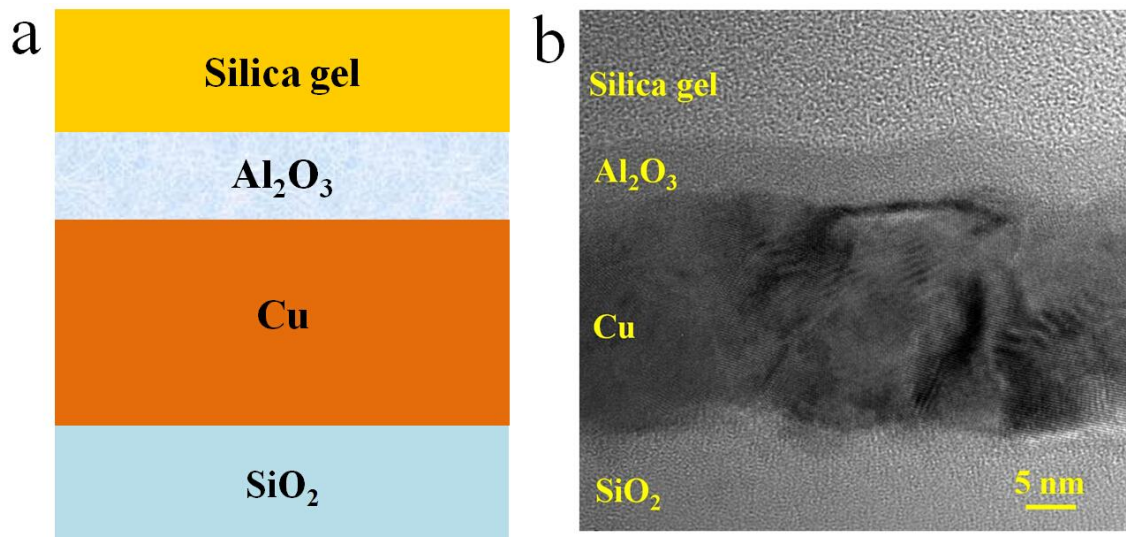


Figure S10.(a) The sample structure for TEM measurement; (b) the HR-TEM image of Cu- Al_2O_3 thin film.

7. The analysis of EQE

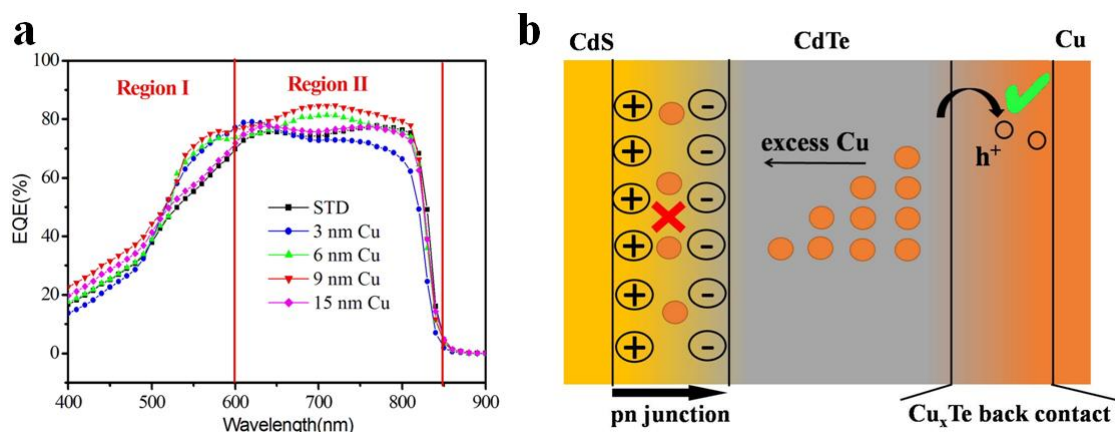


Figure S11 (a) EQE of CdTe solar cell with different Cu thickness on 2 nm ALD-Al₂O₃; (b) The schematic diagram of Cu diffusion mechanism in CdTe solar cell.

The quantum efficiency (QE) of CdTe solar cells was also measured to get insight into the source of the PCE improvement. As shown in **Figure S11a**, it could be divided into two regions, region I (400–600 nm) and region II (600–850 nm). As we know, the QE in region I is greatly dependent on the light absorption, and the production and transport of photon-generated carriers in the CdS/CdTe p-n junction; while the QE in region II is corresponding to the effective transport of photon-generated carriers at the back contact.³ Their correlations were illuminated in **Figure S11b**. When the thickness of Cu film is 3–9 nm, the QEs of cells in region I are higher than that of the standard cell (seen in **Figure S11a**). It could be attributed to the efficient inhibit of excessive Cu diffusion into the p-n junction by the Cu-Al₂O₃ film. When the thickness of Cu film increases to 15 nm, excessive free Cu diffuses into the

p-n junction, which results in the large recombination of photogenerated carriers and directly leads to the decrease of QE in region I. In region II, when the thickness of Cu film was 3 nm, little Cu could cross through Al₂O₃ layer into the CdTe layer to form Cu_xTe back contact, which leads to an obvious decrease of QE compared with the standard cell. When it increase to 6 nm and 9 nm, enough Cu diffuses into the CdTe layer and the Cu_xTe back contact is efficiently constructed, which results into the increase of their QEs. This effective control of Cu diffusion by the ALD-Al₂O₃ film has also been demonstrated by the measurement of carrier lifetime above. In one word, all these data could demonstrate that the Cu diffusion could be effectively controlled by ALD-Al₂O₃ film when adjusting the thickness of Cu film. The best efficiency (13.0%) is achieved by constructing perfect Cu_xTe back contact and eliminating excessive Cu diffusion into the p-n junction meanwhile.

8. The solar cell performance with different Cu annealing treatment.

As known all, the Cu diffusion effect is dependence on the annealing temperature. Therefore, the photocurrent characteristic of three cells with the same thickness of Al₂O₃ and Cu, which exposed to thermal anneal in N₂ glovebox at fixed temperatures (200 °C ,220 °C, 250 °C, 280 °C), were presented in **Figure S12**. It is

shown that the Cu diffusion on the Al_2O_3 layer can make a better performance of solar cell under 250 °C anneal.

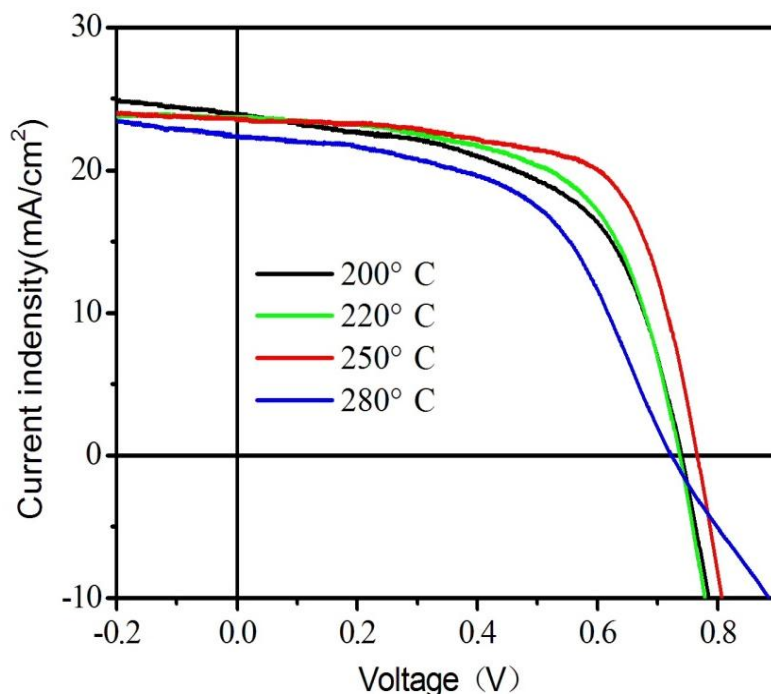


Figure S12. Photocurrent J–V of CdTe cell with different annealing temperature

9. The FTO glass also impacts on the power conversion efficiency of CdTe solar cell.

The highest power conversion efficiency PCE of our solar cell is limit by the FTO glass substrate's transmittance. We have detected the transmittance of our FTO glass substrate by the UV-vis spectrophotometer, and the transmittance is less than 80%, as shown in **Figure S13**, which is lower than most of FTO glass. This is the reason why our solar cells' performance is only 13%. Industry or most research institutes use the FTO glass with the transmittance is higher than 90%.³ If our work uses the same specification glass, the PCE of CdS/CdTe might be about 15%.

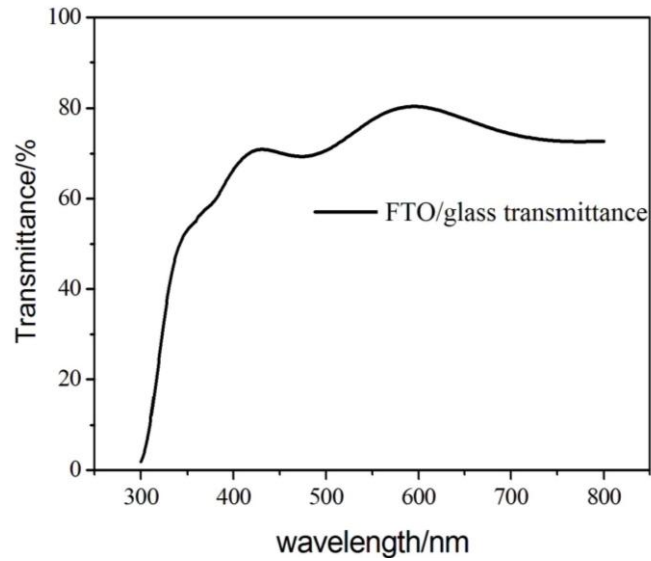


Figure S13. The transmittance of FTO glass detect by UV-vis spectrophotometer.

1. Y. Xuan, H. C. Lin, P. D. Ye and G. D. Wilk, *Appl. Phys. Lett.*, 2006, **88**, 263518.
2. S. T. Tan, B. J. Chen, X. W. Sun, W. J. Fan, H. S. Kwok, X. H. Zhang and S. J. Chua, *J. Appl. Phys.*, 2005, **98**, 013505.
3. K. H. Tsui, Q. Lin, H. Chou, Q. Zhang, H. Fu, P. Qi and Z. Fan, *Adv. Mater.*, 2014, **26**, 2805-2811.